Energy & Environmental Science

Cite this: *Energy Environ. Sci.*, 2011, **4**, 4108

www.rsc.org/ees

PAPER

Reversibility of the hydrogen desorption from $NaBH_4$ by confinement in nanoporous carbon†

Peter Ngene,[a] Roy van den Berg,[a] Margriet H. W. Verkuijlen,[b] Krijn P. de Jong[a] and Petra E. de Jongh*[a]

Received 17th April 2011, Accepted 8th July 2011
DOI: 10.1039/c1ee01481a

$NaBH_4$ is an interesting hydrogen storage material for mobile applications due to its high hydrogen content of 10.8 wt%. However, its practical use is hampered by the high temperatures (above 500 °C) required to release the hydrogen and by the non reversibility of the hydrogen sorption. In this study, we show that upon heating to 600 °C, bulk $NaBH_4$ decomposed into Na and $Na_2B_{12}H_{12}$, releasing the expected 8.1wt% of hydrogen. Nanosizing and confinement of $NaBH_4$ in porous carbon resulted in much faster hydrogen desorption kinetics. The onset of hydrogen release was reduced from 470 °C for the bulk to below 250 °C for the nanocomposites. Furthermore, the dehydrogenated nanocomposites were partially rehydrogenated to form $NaBH_4$, with the absorption of about 43% of the initial hydrogen capacity at relatively mild conditions (60 bar H_2 and 325 °C). Reversibility in this system was limited due to partial loss of Na during dehydrogenation. The dehydrogenated boron compounds were almost fully rehydrogenated to $NaBH_4$ (98%) when extra Na was added to the nanocomposites. To the best of our knowledge, this is the first time that reversibility for $NaBH_4$ has been demonstrated.

Introduction

Solid state hydrogen storage in metal hydrides attracts much attention due to its potential for application in hydrogen fuel cell cars and its advantages in terms of safety and volumetric hydrogen content when compared to high pressure gaseous hydrogen storage.[1,2] A class of compounds that is extensively being investigated as potential hydrogen storage material is the metal borohydrides $M(BH_4)_n$.[3–7] The interest in these materials lies in their stability at room temperature and high hydrogen capacities. $NaBH_4$ is the first known borohydride and has been widely used as a reducing agent in organic chemistry, especially in the reduction of functional groups like aldehydes and ketones into alcohols[8] and more recently in metal colloid synthesis. $NaBH_4$ is relatively stable in air, and has gravimetric and volumetric hydrogen contents of 10.8 wt% and 115 kg of H_2 m^{-3} respectively, fulfilling the capacity requirements for onboard hydrogen storage as set by the US department of energy (DOE). Since its discovery, extensive studies

[a]*Inorganic Chemistry and Catalysis, Debye Institute for Nanomaterials Science, Utrecht University, Universiteitsweg 99, 3584, CG, Utrecht, The Netherlands. E-mail: p.e.dejongh@uu.nl; Fax: +31 30 251 1027; Tel: +31 6 22736345*
[b]*Institute for Molecules and Materials, Radboud University, Heyendaalseweg 135, 6525, AJ, Nijmegen, The Netherlands*

† Electronic supplementary information (ESI) available: Influence of loading on the structure and H_2 desorption properties of the nanocomposite; cycling of the nanocomposites; nitrogen physisorption; NMR results for bulk $NaBH_4$; and equilibrium diagram for $NaBH_4$ decomposition. See DOI: 10.1039/c1ee01481a

Broader context

For hydrogen to be widely used as fuel for vehicles, a compact, safe and cost effective method has to be developed for onboard hydrogen storage. The use of complex hydrides for reversible hydrogen storage in cars is advantageous in terms of safety and hydrogen densities when compared to pressurized and liquefied hydrogen. For example, $NaBH_4$ contains 10.8 wt% H_2 which is ideal for onboard hydrogen storage. Unfortunately its use is hindered by high dehydrogenation temperatures and non reversibility. This work reports that when bulk $NaBH_4$ is heated to 600 °C in Ar flow, it decomposes irreversibly into Na and $Na_2B_{12}H_{12}$ releasing 8.1 wt% H_2. Nanoconfinement of $NaBH_4$ in nanoporous carbon decreased the onset of dehydrogenation to below 250 °C (470 °C for bulk $NaBH_4$), and also resulted in the first observation of reversible formation of $NaBH_4$ from the dehydrogenation products at relatively mild conditions (325 °C and 60 bar H_2). Although these conditions are still far from the requirements for practical application, our work shows that we can fundamentally change hydrogen release temperatures and reversibility in a very stable material like $NaBH_4$. This demonstrates the strength of nanoconfinement in carbon as an approach towards reversible hydrogen storage materials.

have been undertaken on the use of $NaBH_4$ as a hydrogen storage material. Most of these studies focussed on hydrogen release *via* catalyzed hydrolysis of $NaBH_4$.[8,9] However, DOE recently recommended a no-go for $NaBH_4$ hydrolysis as a hydrogen source for vehicular applications due to the formation of stable $NaBO_2$ that can not be recycled efficiently.[10]

An alternative method to release the hydrogen from $NaBH_4$ is by thermal decomposition into H_2, B and Na (or NaH).[11–14] However, like most alkali borohydrides, $NaBH_4$ is thermodynamically very stable (standard enthalpy of formation $\Delta_f H^0 = -188.6$ kJ per mol $NaBH_4$ and entropy of formation $S^0 = 101.3$ JK^{-1} per mol $NaBH_4$)[15] and releases hydrogen only when heated to temperatures exceeding 500 °C[12,13,16,17] which is too high for practical applications in hydrogen fuel cell cars. Furthermore, reversibility of the hydrogen desorption which is a very important criterium for a hydrogen storage material, has never been reported for $NaBH_4$ as far as we are aware.

For $LiBH_4$, a compound similar to $NaBH_4$, the thermal hydrogen sorption properties have been widely investigated and the kinetics of its hydrogen release and uptake improved using techniques such as destabilization, nanosizing/nanoconfinement, and the addition of catalysts.[18–30] However only few reports in literature exists on the thermal hydrogen sorption properties of $NaBH_4$ and they mainly focus on mixtures of $NaBH_4$ and other hydrides, especially MgH_2.[16,31–35] Martelli *et al.*[12] recently studied the stability and decomposition of $NaBH_4$ and reported that the compound decomposes in one step (unlike other complex metal hydrides such as $NaAlH_4$ and $LiBH_4$) to Na and an unidentified boron rich phase. However no further report was made on the identification of the composition of the boron rich phases and no reversibility of the hydrogen desorption from the bulk $NaBH_4$ was reported.

The reversibility of the hydrogen desorption from metal hydrides can be improved by reducing their particle sizes to the nanoscale,[36] which is usually achieved by mechanical milling.[37] However in the case of $NaBH_4$, it has been shown that ball milling is not effective in nanostructuring the compound due to its high structural stability even under heavy deformation conditions imposed by milling.[38] Nanosizing and/or confinement in nanoporous materials (especially carbon) is a new approach which has been shown to significantly improve the hydrogen uptake kinetics (and in some cases also the thermodynamics) of complex hydrides.[22,36,39–44] Ampoumogli *et al.*[45] recently synthesized $NaBH_4$/carbon nanocomposites *via* impregnation of porous carbon with $NaBH_4$ dissolved in liquid ammonia and showed that the nanocomposites releases hydrogen at lower temperatures than bulk $NaBH_4$. However, the hydrogen release was associated with ammonia and no reversibility was observed in this nanocomposite.

In this work, we study the thermal hydrogen release from $NaBH_4$ and investigate how confinement of $NaBH_4$ in nanoporous carbon using different preparation routes affects the hydrogen sorption properties. Our study reveals that $NaBH_4$ decomposes into metallic Na, $Na_2B_{12}H_{12}$ and H_2 rather than into Na or NaH, B and H_2 as postulated earlier.[13,46] In addition, we show that confining $NaBH_4$ in nanoporous carbon resulted in a significant increase in the dehydrogenation kinetics and remarkably enabled the rehydrogenation of the decomposition products to $NaBH_4$ at relatively mild conditions.

Experimental

$NaBH_4$/C nanocomposites were prepared using pore volume impregnation with an aqueous $NaBH_4$ solution (denoted SI) or melt infiltration (MI). For pore volume impregnation, 1.1g $NaBH_4$ (98+% pure, Acros Organics) was dissolved in 2 ml water of pH 13, which was prepared by adding 0.3 g NaOH (Merk 99%) to 10 ml demineralized water. 1g of high surface area carbon (HSAG-500, Timcal Ltd., pore volume 0.66 cm^3 g^{-1}, BET surface area 500 m^2 g^{-1}, broad pore size distribution dominated by 2–3 nm pores) that had been previously dried overnight under vacuum at 200 °C was impregnated with 0.66 ml of the $NaBH_4$ solution. The water in the impregnated sample was removed by drying overnight at 165 °C under vacuum (~9 mbar). The impregnation and drying were done using a Schlenk technique while $NaBH_4$ handling and storage was conducted under Ar atmosphere in a glovebox (<0.1 ppm of O_2 and H_2O). For melt infiltration, the required amounts of carbon (which had been dried) and $NaBH_4$ were mixed in a graphite sample holder and placed in stainless steel autoclave. The mixture was heated under hydrogen atmosphere at 5 °C/min to 520 °C (melting point of $NaBH_4 \sim 500$ °C) and dwelled at 520 °C for 25 min at approximately 5 bar H_2. Nanocomposites containing various compositions of $NaBH_4$ and C were synthesized and labeled according to the weight percentage of $NaBH_4$ in the composite. As a reference, physically mixed samples of $NaBH_4$ and C or graphite (BET surface area 7 m^2 g^{-1}) were prepared by mixing the required amounts in a mortar using a pestle.

Structural characterization was performed using X-ray diffraction (XRD), N_2- physisorption and both ^{11}B and ^{23}Na solid-state Nuclear Magnetic Resonance (NMR) spectroscopy. All measurements were done in air tight sample holders. XRD patterns were obtained at room temperature from 18 to 80° 2θ with a Bruker-AXS D-8 Advance X-ray diffractometer setup using $CoK\alpha_{1,2}$ radiation with $\lambda = 1.79026$ Å. N_2-physisorption measurements were performed at −196 °C, using a Micromeritics Tristar 3000 apparatus. The pore size distributions of the samples were calculated from the desorption branch using BJH theory with the Harkins and Jura thickness equation. Solid-state NMR experiments were performed on a 600 MHz Varian spectrometer using a 2.5 mm HX MAS probe. ^{11}B and ^{23}Na single pulse excitation spectra were obtained using a short hard pulse of 0.20 μs at an effective rf-field strength of 140 kHz after taking pulse rise and decay times into account. Spectra were acquired without proton decoupling. A sample spinning speed of 15 kHz was applied. The ^{11}B spectra were referenced using an aqueous solution of H_3BO_3 as secondary reference with a chemical shift of $\delta = 19.6$ ppm relative to $BF_3 \cdot OEt_2$ ($\delta = 0$ ppm). The ^{23}Na spectra were referenced with respect to an aqueous solution of NaCl ($\delta = 0$ ppm).

Hydrogen release from the samples was measured by temperature programmed desorption (TPD) using a Micromeritics AutoChem II 2920 apparatus. 100 to 150 mg of sample was heated at 5 °C/min from room temperature to 450–600 °C in 25 ml/min Ar (99.99% purity) flow with a dwell time of 25 min at the maximum temperature. The composition of the desorbed gas was analyzed using a quadrupole mass spectrometer (Pfeifer) attached to the TPD gas outlet. Rehydrogenation of desorbed samples was performed in an autoclave at 60 bar H_2 and 325 °C for 5 h after which the amount of H_2 absorbed by the sample was

determined by a second TPD run. Cycling of the sample was performed in a magnetic suspension balance from Rubotherm. About 100 mg of the sample was loaded in a graphitic cup and inserted into a stainless steel sample holder. The sample was heated at 5 °C/min to 400 °C in 25 ml/min Ar flow. Rehydrogenation of the desorbed sample was performed at 325 °C by increasing the H_2 pressure from zero to 60 bar in 60 min and remaining at this pressure and temperature for 5 h. Hydrogen uptake and release were determined from the weight changes after having corrected for buoyancy effects.

Results and discussion

Structure of the $NaBH_4$/C nanocomposites

The X-ray diffraction (XRD) patterns of a physical mixture of 25 wt% $NaBH_4$ and nanoporous carbon, and 25 wt% $NaBH_4$/C nanocomposites prepared through solution impregnation (SI) and melt infiltration (MI) are shown in Fig. 1. The XRD pattern of the carbon shows two diffraction lines at 31° (002) and around 52° (10) 2θ that are typical for turbostratic graphitic materials. After synthesis, all diffraction lines can be ascribed to either carbon or $NaBH_4$. A comparison of the diffraction patterns of the physical mixture and the nanocomposites show a clear broadening and a huge reduction in the intensity of $NaBH_4$ diffraction lines in the nanocomposites. A decrease in the amount of $NaBH_4$ in the nanocomposites to 20 and 15 wt% led to nanocomposites with no detectable diffraction from the $NaBH_4$ (see Fig. S1 in the electronic supplementary information ESI†). Similar observations have been reported for $LiBH_4$ confined in porous carbon and silica, and were attributed to a decrease in the long-range order of the compound due to nanozing and confinement in the porous hosts.[28,29] Hence, we conclude that the $NaBH_4$ is confined in the porous carbon.

Further evidence for the incorporation of the $NaBH_4$ into the pores of the carbon is from nitrogen physisorption measurements (Fig. 2) which show that the total pore volume of the carbon decreased from 0.64 cm^3/g C in the PM sample to 0.31 and 0.24 cm^3/g C in the solution impregnated and melt infiltrated nanocomposites respectively. This decrease in pore volume (0.33 cm^3/g C in SI and 0.40 cm^3/g C in the MI) is close to the volume of $NaBH_4$ (0.31cm^3) added in the mixture, in agreement with the fact that the $NaBH_4$ is in the pores of the carbon. The slight difference is most likely due to minor pore blocking and some pore loss (≈ 0.05 cm^3/g) during heat treatment.

Hydrogen release

Fig. 3 shows the hydrogen release from bulk $NaBH_4$, a physical mixture of 25wt% $NaBH_4$ and porous carbon (PM), and the MI and SI 25wt% $NaBH_4$/C nanocomposites. Hydrogen release started in the bulk $NaBH_4$ around 470 °C with two major peaks at 515 °C and 560 °C, in line with literature.[13] The onset of hydrogen release is significantly lower (about 320 °C) for the PM sample than for the bulk $NaBH_4$. However, hydrogen release also occurred partially around 500 °C which is the melting point of $NaBH_4$. For the MI nanocomposite, hydrogen release started at much lower temperatures (below 300 °C) and the majority of the hydrogen was released around 450 °C. Remarkably, for the impregnated sample hydrogen release started below 250 °C, about 220 °C lower in temperature than bulk $NaBH_4$ and with a maximum release rate at 350 °C which is in agreement with a previous report for $NaBH_4$/C nanocomposites synthesized *via* impregnation of $NaBH_4$/liquid ammonia solution.[45] These observations clearly demonstrate that nanoconfinement in porous carbon enhances the dehydrogenation of $NaBH_4$ significantly. The difference in the hydrogen release temperatures of the MI and SI samples suggests the presence of different $NaBH_4$ feature sizes in the two samples which might be due to differences in the interaction of carbon with molten $NaBH_4$ and aqueous $NaBH_4$ solution. Lowering the loading of $NaBH_4$ in the MI nanocomposites led to hydrogen release at lower temperatures, similar to those for the SI sample (Fig. S2†).

Qualitative analysis of the desorbed gas using mass spectrometry (not shown) proved that hydrogen was released in all cases and if other gases were released, the amount was below the detection limit (5E-11 ion current [A]).

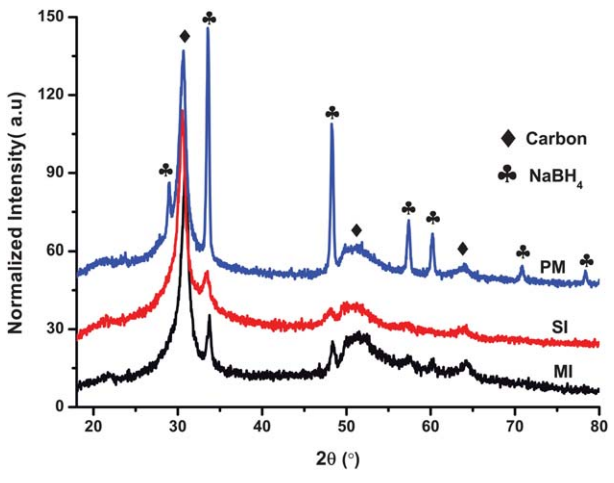

Fig. 1 XRD Pattern of a physical mixture of 25wt% $NaBH_4$ and carbon (PM), and 25 wt% $NaBH_4$/C nanocomposites synthesized *via* melt infiltration (MI), solution impregnation (SI).

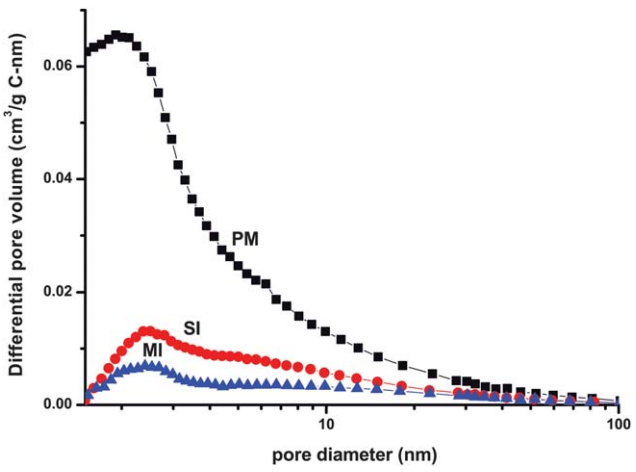

Fig. 2 Differential pore volume *versus* pore diameter for a physical mixture of $NaBH_4$ and carbon (PM), solution impregnated (SI) and melt infiltrated (MI) $NaBH_4$/C nanocomposites, showing loss of carbon porosity upon $NaBH_4$ incorporation.

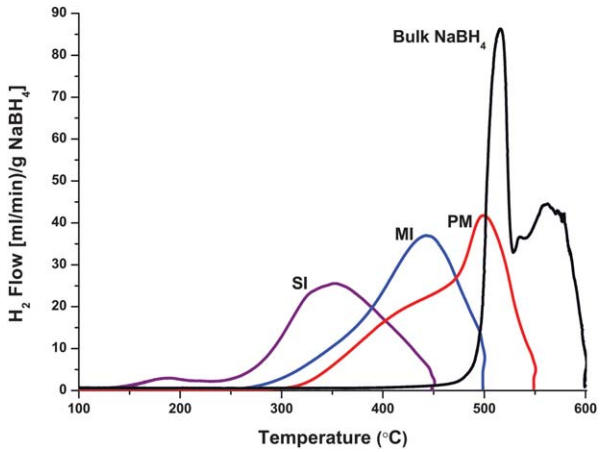

Fig. 3 Temperature Programmed Desorption- TPD while heating with 5 °C/min in Ar flow, showing hydrogen release from the bulk, a physical mixture of 25 wt % $NaBH_4$ and porous carbon (PM), solution impregnated (SI) and melt infiltrated (MI) 25 wt% $NaBH_4$/C nanocomposites.

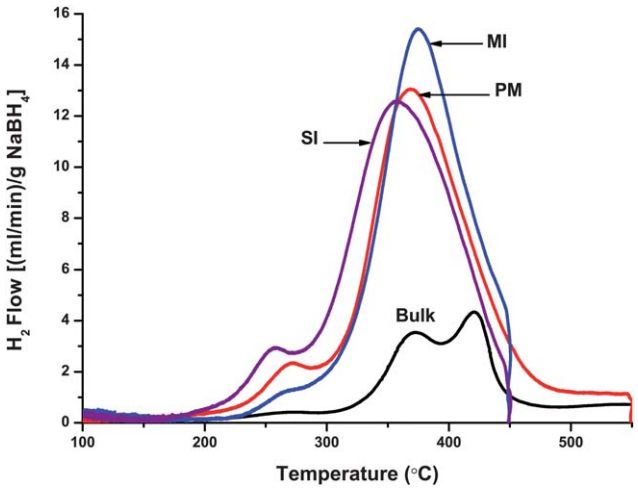

Fig. 4 Hydrogen release from the rehydrogenated bulk $NaBH_4$, physically mixed (PM), melt-infiltrated (MI) and solution impregnated (SI) nanocomposites. Rehydrogenation was done under 60 bar H_2 and 325 °C for 5 h.

The SI nanocomposite released approximately 6.7 wt% H_2 (normalized to the $NaBH_4$ content) after heating to 450 °C and dwelling for 25 min, the MI nanocomposites released 7.9 wt% H_2/g $NaBH_4$ (≈ 2.1wt% H_2/g sample) with same dwell time at 500 °C, while 8.1 wt% H_2 was released in the physically mixed sample and the bulk $NaBH_4$ after heating to 600 °C and dwelling for 25 min. The minor difference in hydrogen release for the nanocomposites and the physical mixtures is most likely due to partial decomposition or oxidation of the sample during synthesis and handling. Decomposition of $NaBH_4$ into NaH and B would release 8.1 wt% H_2 while 10.8 wt% H_2 would be expected for decomposition into elemental Na and B.

Reversibility

Reversibility of the hydrogen desorption in the composites was evaluated by rehydrogenating the dehydrogenated samples in an autoclave at 325 °C and 60 bar H_2 for 5 h. The hydrogen release from the rehydrogenated samples is shown in Fig. 4. About 0.9 wt % hydrogen was released from the rehydrogenated bulk $NaBH_4$ indicating minor hydrogen uptake during rehydrogenation. Remarkably, the nanocomposites and the physically mixed $NaBH_4$/porous C released about 3.4 wt% H_2/g $NaBH_4$, indicating about 43% reversibility under these mild conditions. As far as we are aware, this is the first report of a successful rehydrogenation of $NaBH_4$ decomposition products. Furthermore, the nanocomposites can be cycled repeatedly as shown in Fig. S3,† although the capacity decreases steadily as in the case of nanoconfined $LiBH_4$.[22] These results show that confinement in the pores of the carbon plays an important role in determining reversibility. The reversibility seen in the physically mixed sample (PM) results from the fact that $NaBH_4$ melts (500 °C) during the first cycle desorption and infiltrates the pores of the carbon thereby forming nanoconfined products after decomposition that can be rehydrogenated. This is confirmed from nitrogen physisorption measurements which show that the total pore volume of carbon decreased by 0.26 cm^3/g after dehydrogenation (Fig. S4†). Such reversibility was not observed for a similar experiment with non porous carbon or graphite (data not shown).

Notably, all the rehydrogenated nanocomposites released hydrogen in the same temperature range, which means that the desorption temperatures especially for the MI nanocomposites had shifted to lower values. This suggests a possible microstructural change and/or redistribution of the $NaBH_4$ in the carbon after rehydrogenation. The bulk $NaBH_4$ shows some reversibility (≈ 0.9 wt% H_2 released) but only if the first desorption cycle is done in a closed system.

To investigate structural changes occurring in the samples during dehydrogenation and rehydrogenation processes, XRD patterns of the dehydrogenated and rehydrogenated samples were acquired (Fig. 5) and compared to the pure $NaBH_4$. For bulk $NaBH_4$, we physically observed two distinct solid phases after dehydrogenation as recently reported for dehydrogenated bulk $NaBH_4$.[12] However XRD showed peaks predominantly from Na, with a minor unidentified phase as evidenced by a small peak at 45° (2θ). After rehydrogenation, two distinct phases were still physically observed but only NaH was detected from the XRD, showing that for the bulk $NaBH_4$, part of the de- and rehydrogenated material is amorphous.

For both nanocomposites (MI and SI), only C diffraction peaks were observed after hydrogen desorption indicating that the desorption products are amorphous. After rehydrogenation, in addition to the C, diffraction peaks due to $NaBO_2$ were observed in the impregnated nanocomposites. The $NaBO_2$ is probably due to reaction between NaOH (used to stabilize the $NaBH_4/H_2O$ solution) and $NaBH_4$ or its decomposition products at high temperatures. In contrast, no diffraction peaks other than that from the C were observed for the melt infiltrated samples. This shows that for both samples, the hydrogenated phases are amorphous as also reported in literature for $LiBH_4$ and $NaAlH_4$ confined in porous carbon.[22,28,39,47]

Characterization of the non crystalline phases

A convenient technique to investigate the local structure of non-crystalline solids is solid-state magic angle spinning (MAS)

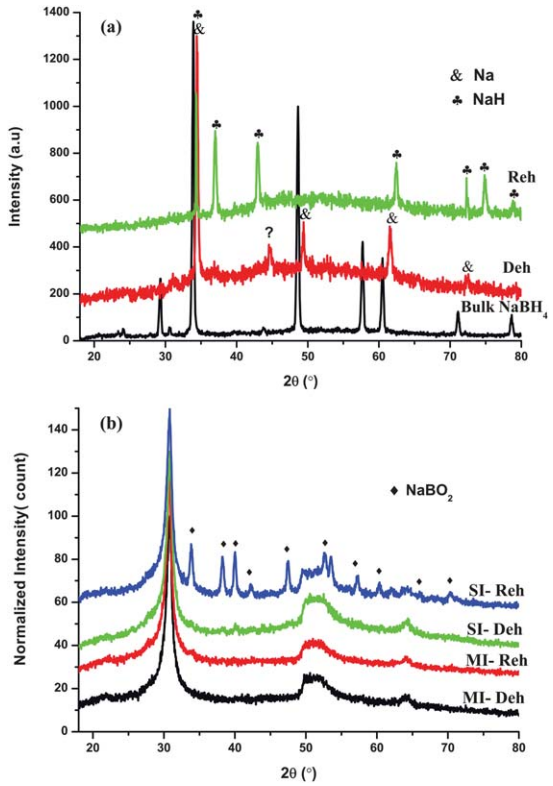

Fig. 5 XRD pattern of (a): Bulk $NaBH_4$ at room temperature and after dehydrogenation (Deh) and rehydrogenation (Reh). (b): the melt infiltrated (MI) and solution impregnated (SI) 25wt% $NaBH_4$/C nanocomposites after dehydrogenation and rehydrogenation.

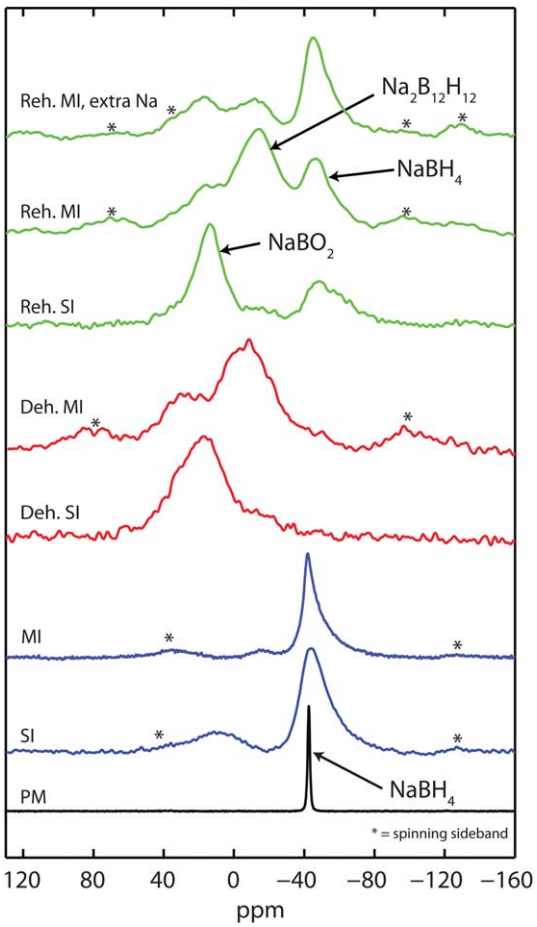

Fig. 6 Solid-state ^{11}B MAS-NMR spectra of samples containing 25 wt% $NaBH_4$ and porous carbon: (PM) Physical mixture; (SI) Sample prepared by solution impregnation; (MI) Sample prepared by melt infiltration; (Deh. SI) Sample SI after dehydrogenation; (Deh. MI) Sample MI after dehydrogenation; (Reh. SI) Sample SI after rehydrogenation; (Reh. MI) Sample MI after rehydrogenation, (Reh. MI, extra Na) MI sample containing extra Na. Asterisks indicate spinning sidebands.

NMR. Fig. 6 shows the ^{11}B NMR spectra of a physical mixture of $NaBH_4$ and porous carbon, and the nanocomposites after synthesis, dehydrogenation and rehydrogenation. The ^{11}B spectrum of a physical mixture of $NaBH_4$ and porous carbon shows a well defined sharp peak at −42.6 ppm. For the nanocomposites (both melt infiltrated and volume impregnated), the lineshape of $NaBH_4$ is broadened. As reported previously for $NaAlH_4$/C nanocomposites,[47,48] this line broadening is explained by distortions of the local field homogeneity because of the magnetic susceptibility of the carbon and/or a higher disorder in the material, which results in a distribution in chemical shift and quadrupolar interaction parameters. The impregnated nanocomposite exhibits a significantly larger linewidth with a full width at half maximum (FWHM) of 17.1 ppm compared to the melt infiltrated sample with a FWHM of 9.4 ppm. This means that the microstructure and/or distribution over the carbon depends on the preparation method as was also clear from the physisorption and hydrogen release measurements.

After dehydrogenation, all $NaBH_4$ disappeared in both MI and SI samples. For the dehydrogenated SI sample, a large resonance peak with a maximum at 16 ppm is present. ^{11}B has typical isotropic chemical shifts between 12 and 19 ppm in materials with trigonal B–O coordination.[49–51] Hence this peak can be assigned to $NaBO_2$ in agreement with the XRD results. The dehydrogenated MI sample shows mainly a broad resonance with a maximum at −13 ppm which is assigned to $Na_2B_{12}H_{12}$.[52–54] The smaller contribution at 18 ppm corresponds most likely to $NaBO_2$. In the sample after melt infiltration, a small amount of $Na_2B_{12}H_{12}$ is also observed which is most likely due to partial desorption, or reaction between $NaBH_4$ and minor impurities in the carbon during melt infiltration. No clear evidence of the formation of elemental boron is found. Boron gives a broad line around 5 ppm[55] and therefore, its resonance might overlap with the resonances of $Na_2B_{12}H_{12}$ and/or $NaBO_2$.

After rehydrogenation, in both samples nanoconfined $NaBH_4$ is reformed. This clearly proves the partial reversibility for these nanocomposites. Clear differences exist between the MI and SI samples. Besides nanoconfined $NaBH_4$, the MI samples show mainly $Na_2B_{12}H_{12}$ and little $NaBO_2$, while the SI samples show mainly $NaBO_2$ and only a minor amount of $Na_2B_{12}H_{12}$. The linewidth of the $NaBH_4$ resonance increased slightly after rehydrogenation especially for the MI sample. This suggests a possible change in the structure and/or distribution of $NaBH_4$ in the carbon after rehydrogenation and is most likely responsible for the rehydrogenated MI sample (Reh. MI) when compared to the as synthesized sample (MI).

Similar to the MI sample, ^{11}B NMR of the dehydrogenated bulk $NaBH_4$ show a broad resonance that is mainly due to $Na_2B_{12}H_{12}$ (Fig. S5†) and minor traces of unreacted $NaBH_4$. However in contrast to the nanocomposites, $NaBH_4$ was not reformed after rehydrogenation of the dehydrogenated bulk $NaBH_4$.

^{23}Na NMR of the samples was also measured in order to investigate the evolution of the Na phase(s). Unfortunately, for the nanocomposites, ^{23}Na NMR gave very broad spectra from which no useful information about the Na phases could be extracted. In general, the chemical shift range for ^{23}Na is relatively small (~30 ppm) compared to ^{11}B, which results in an overlap of the resonances of different compounds especially when the peaks are broad. This broadening is most likely caused by the high dispersion of Na when confined and in close contact with the carbon. Meanwhile ^{23}Na NMR for the bulk $NaBH_4$ (Fig. S6†) shows resonances due to elemental Na and $Na_2B_{12}H_{12}$ after dehydrogenation. After rehydrogenation, the Na resonance disappears while $Na_2B_{12}H_{12}$ and a peak at a chemical shift due to NaH are clearly seen, in agreement with the XRD results. The formation of NaH (instead of $NaBH_4$) after the rehydrogenation of the bulk $NaBH_4$ explains the differences in the hydrogen release profile from the rehydrogenated nanocomposites and the rehydrogenated bulk sample.

Addition of extra sodium

The reversibility achieved in the nanoconfined $NaBH_4$ is relatively low when compared to that of other complex hydrides such as $NaAlH_4$ and $LiBH_4$ confined in similar carbon materials.[22,40,56] Apart from partial oxidation of the sample during handling (which also occurs in other nanoconfined hydrides), two major reasons could be responsible for the partial reversibility. Firstly, XRD and NMR measurements clearly show that elemental Na and $Na_2B_{12}H_{12}$ are the main dehydrogenation products of $NaBH_4$. The predicted high stability of $Na_2B_{12}H_{12}$ could prevent the rehydrogenation to $NaBH_4$, as recently postulated.[54] Secondly, since Na is liquid and has a relatively high vapour pressure at 500 °C, the loss of Na through evaporation during dehydrogenation of $NaBH_4$ is likely (Fig S7). In that case there will be insufficient Na to fully form $NaBH_4$ from the dehydrogenated boron compounds. To check if this latter assumption is true, extra Na was added to the melt infiltrated nanocomposites by heating a 20wt% $NaBH_4$/C nanocomposite with 12.5 wt% NaH (95%, Aldrich). The overall composition of the mixture is 17.5, 70 and 12.5 wt% $NaBH_4$, C and NaH respectively (molar ratio Na: B = 2.1). It is expected that Na formed after the dehydrogenation of the NaH will infiltrate the pores of the carbon as previously reported,[57] thereby providing extra Na to the dehydrogenated nanocomposites. After dehydrogenation, the samples were rehydrogenated at 325 °C and 60 bar H_2 for 5 h. Fig. 7 shows the second hydrogen release run. The 20wt% $NaBH_4$/C nanocomposite released approximately 0.7 wt% H_2/g sample (3.5 wt% H_2/g $NaBH_4$). The nanocomposite containing extra Na released 1.4 wt% H_2/g sample (8.0 wt% H_2/g $NaBH_4$), while 8.1 wt% H_2/g $NaBH_4$ is expected for fully reversible decomposition to $Na_2B_{12}H_{12}$.

One has to consider that the additional Na could also have been rehydrogenated, and contribute to the hydrogen release.

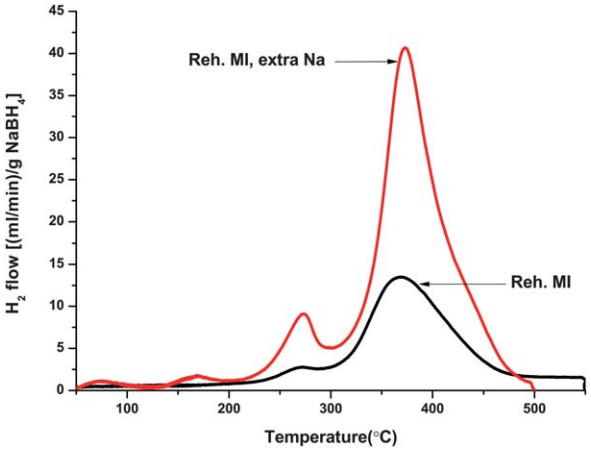

Fig. 7 H_2 release from rehydrogenated sample of 20 wt% $NaBH_4$/C nanocomposite (Reh. MI) and a 20wt% $NaBH_4$/C nanocomposite containing extra Na; molar ratio of Na: B = 2.1 (Rh. MI, extra Na).

However, the additional NaH could contribute a maximum of 0.55 wt % H_2 per gram nanocomposite, and hence never fully account for the increase in reversibility. More importantly, ^{11}B NMR of the rehydrogenated sample (Fig. 6) shows a large increase in the resonance due to $NaBH_4$ in the sample with extra Na, as well as fading of the resonance due to $Na_2B_{12}H_{12}$. This proves that in these nanoconfined systems neither B nor $Na_2B_{12}H_{12}$ are intrinsically limiting factors for the reversibility of hydrogen sorption. Nearly full reversibility could be obtained by compensating for the loss of active Na from the system. Alternatively, loss of Na might be reduced by restricting operation temperatures and gas flow.

Discussions

Most alkali metal borohydrides decompose to the metal hydride before further decomposition to the metal, although direct decomposition into the element is also possible. Thus for the dehydrogenation of $NaBH_4$ the following overall reaction equations can be written:

$$2\ NaBH_4 \rightarrow 2\ NaH + 2\ B + 3\ H_2 \quad (1)$$

$$NaBH_4 \rightarrow Na + B + 2\ H_2. \quad (2)$$

Decomposition according to reaction 1 releases 8.1 wt% H_2 while reaction 2 yields 10.8 wt% H_2. Experimentally, bulk $NaBH_4$ released 8.2 wt% H_2 while the MI-nanocomposite and the physically mixed samples released approximately 8.1 wt% H_2/[$NaBH_4$] which would suggest that these samples decomposed according to reaction 1. However, the lower stability of NaH compared to $NaBH_4$ implies that NaH should already decompose at lower temperatures than required for the decomposition of $NaBH_4$[58,59] especially in the presence of carbon.[57] Furthermore, the NMR results clearly show that the decomposition products of $NaBH_4$ are mostly $Na_2B_{12}H_{12}$ and Na. These observations suggest that only partial decomposition of $NaBH_4$ takes place according to the following overall reaction equation:

$$12\ NaBH_4 \rightarrow 10\ Na + Na_2B_{12}H_{12} + 18\ H_2 \quad (3)$$

Interestingly, decomposition according to (3) is expected to yield 8.1 wt% H_2 which is in a good agreement with the amount of hydrogen released from the samples. The presence of two desorption steps in the bulk $NaBH_4$ and in all the rehydrogenated nanocomposites could be due to either an intermediate decomposition product, or heterogeneity of the $NaBH_4$.

For the solution impregnated sample, formation of $NaBO_2$ is observed with both XRD and NMR. As NaOH is present, this can probably be explained by the following reaction:

$$NaBH_4 + 2\ NaOH \rightarrow NaBO_2 + 2\ Na + 3\ H_2 \qquad (4)$$

Since the molar ratio of $NaBH_4$ to NaOH in the aqueous $NaBH_4$ solution is 20 : 1, only about 2.5% of the $NaBH_4$ is consumed in this reaction (except if traces of water are still present in the sample). Unlike for the MI sample, no clear resonance due to $Na_2B_{12}H_{12}$ was observed with NMR after dehydrogenation. The reversibility seen in the SI sample shows that phases other than oxidation products must be present after dehydrogenation since $NaBO_2$ cannot be rehydrogenated to $NaBH_4$. Unfortunately, neither elemental B nor other boron compounds can clearly be identified with solid-state NMR due to possible overlap of these resonances with the broad $NaBO_2$ resonance. The microstructure and/or distribution of the $NaBH_4$ over the carbon depend on the preparation method, as seen from NMR and nitrogen physisorption results. Also Fig. 3 shows different hydrogen release profiles for SI and the MI nanocomposites. However, at present we cannot identify which boron species are reversibly formed after dehydrogenation in the SI samples.

Remarkable is the reversible formation of $NaBH_4$ in these nanocomposites especially at such mild conditions as used in this study since for $NaBH_4$ reversible hydrogen sorption has not yet been reported. Reversibility in complex hydrides especially borohydrides is typically hampered by the formation of at least two crystalline or amorphous phases after desorption which are the metal or metal hydride phase and boron/boron species. Bulk $NaBH_4$ forms crystalline Na and amorphous $Na_2B_{12}H_{12}$ after desorption. Reversibility in such a system is difficult because of the slow solid state diffusion required for the recombination of these macroscopically segregated phases. This is evidenced by the fact that after rehydrogenation, NaH and $Na_2B_{12}H_{12}$ were seen instead of $NaBH_4$. This suggests that NaH is first formed during rehydrogenation and since it is a solid at the rehydrogenation conditions, it did not react with the $Na_2B_{12}H_{12}$ to form $NaBH_4$. Furthermore, Caputo *et al.* recently calculated that $Na_2B_{12}H_{12}$ is very stable (standard enthalpy of formation at 0 K = −1086 kJ/mol $Na_2B_{12}H_{12}$ or −181 kJ/mol H_2) and cannot be rehydrogenated if formed during dehydrogenation of $NaBH_4$.[54] However, the results presented in this study clearly showed that nanoconfined $NaBH_4$ exhibits partial reversible hydrogen sorption and that full reversibility can be achieved if Na is not lost during dehydrogenation. Therefore the barrier to reversibility in bulk $NaBH_4$ is not due to the stability of $Na_2B_{12}H_{12}$ but rather due to the inability of NaH (formed during rehydrogenation) and $Na_2B_{12}H_{12}$ to react with H_2 to form $NaBH_4$ at moderate conditions because of phase separation and poor kinetics of solid-state diffusion required for their recombination. Furthermore, bulk $NaBH_4$ decomposes above 500 °C and Na loss through evaporation at this high temperatures (except when desorption is carried in a closed system) practically hinders the reversibility of the dehydrogenation reaction. Confining the $NaBH_4$ in nanoporous carbon reduces these problems. When confined, the dehydrogenated phases are kept together in the pores of the carbon. Therefore the diffusion distance between the Na and $Na_2B_{12}H_{12}$ is greatly reduced, enabling the reversible formation of $NaBH_4$ from its dehydrogenated products even at relatively mild conditions without a catalyst.

Our work clearly demonstrate how the kinetics of hydrogen release from $NaBH_4$ can be greatly enhanced and reversibility enabled by nanosizing and nanoconfinement in carbon. Preliminary investigations also indicate that under 1 bar H_2 pressure, part of the hydrogen is already released starting from 280 °C which is below the temperature at which the dehydrogenation reaction of $NaBH_4$ would be expected in equilibrium.[12] This indicates that the enthalpy and/or entropy for the decomposition reaction might be different for nanoconfined $NaBH_4$ compared to bulk material, or the presence of intermediate decomposition steps for $NaBH_4$ which is different when confined in nanoporous carbon but the details are outside the scope of the present paper.

Despite the fact that the hydrogen release temperatures are lowered and reversibility is observed when $NaBH_4$ is confined in nanoporous carbon, for practical application in fuel cell cars, further reduction in the desorption temperatures to about 150 °C is required in order to avoid Na loss. In addition, the $NaBH_4$ loading must be increased to above 60 wt% in order to increase the overall hydrogen content of the nanocomposite. The latter might be achieved by using nanoporous hosts with higher pore volume.

Conclusions

The thermal hydrogen sorption properties of $NaBH_4$ have been investigated. XRD, solid-state NMR and hydrogen release measurements revealed that $NaBH_4$ decomposes into elemental Na and $Na_2B_{12}H_{12}$ when heated to 600 °C, with a release of 8.1 wt % H_2. $NaBH_4$ was successfully confined into a nanoporous carbon material through impregnation with an aqueous $NaBH_4$ solution and also by melt infiltration under hydrogen pressure. Confining $NaBH_4$ in nanoporous carbon material lowers the desorption temperatures significantly, with most of the hydrogen released around 350 °C(in Ar flow) in the solution impregnated nanocomposites compared to 560 °C for the bulk material. Remarkably, reversible formation of $NaBH_4$ from its dehydrogenation products was demonstrated for the first time as the dehydrogenated $NaBH_4$/C nanocomposites can be rehydrogenated to $NaBH_4$ at relatively mild conditions of 325 °C and 60 bar H_2 for 5h. Reversibility of the system is limited by loss of Na at high temperatures during hydrogen release. Compensation of Na loss by extra Na resulted in almost full rehydrogenation of the dehydrogenated products to $NaBH_4$. Although at the moment $NaBH_4$/C nanocomposites do not meet the requirements for onboard applications, our work demonstrates the strength of nanoconfinement in carbon materials as an approach towards reversible hydrogen storage materials.

Acknowledgements

We would like to thank M. van Zwienen, A. van der Eerden and A. Mens for their technical support. We thank Timcal Ltd. Switzerland for providing the high surface area graphite, and NWO-Vidi Netherlands, 016.072.316 for financial support. The Netherlands Organisation for Scientific Research (NWO) is acknowledged for its support of the solid-state NMR facility for advanced materials research at Radboud University. Finally we thank Prof. Arno Kentgens and Dr Jan van Bentum of Radboud University, Nijmegen for their support regarding the NMR results.

Notes and references

1 L. Schlapbach and A. Züttel, *Nature*, 2001, **414**, 353–358.
2 J. Yang, A. Sudik, C. Wolverton and D. J. Siegel, *Chem. Soc. Rev.*, 2010, **39**, 656–675.
3 A. Züttel, A. Borgschulte and S.-I. Orimo, *Scr. Mater.*, 2007, **56**, 823–828.
4 Y. Nakamori, H. W. Li, K. Miwa, S. Towata and S. Orimo, *Mater. Trans.*, 2006, **47**, 1898–1901.
5 S. Orimo, Y. Nakamori and A. Züttel, *Mater. Sci. Eng., B*, 2004, **108**, 51–53.
6 R. Cerny, Y. Filinchuk, H. Hagemann and K. Yvon, *Angew. Chem., Int. Ed.*, 2007, **46**, 5765–5767.
7 K. Miwa, M. Aoki, T. Noritake, N. Ohba, Y. Nakamori, S. Towata, A. Zuttel and S. Orimo, *Phys. Rev. B*, 2006, **74**.
8 H. I. Schlesinger, H. C. Brown, A. E. Finholt, J. R. Gilbreath, H. R. Hoekstra and E. K. Hyde, *J. Am. Chem. Soc.*, 1953, **75**, 215–219.
9 S. C. Amendola, P. Onnerud, M. T. Kelly, P. J. Petillo, S. L. Sharp-Goldman and M. Binder, *J. Power Sources*, 1999, **84**, 130–133.
10 U. B. Demirci, O. Akdim and P. Miele, *Int. J. Hydrogen Energy*, 2009, **34**, 2638–2645.
11 D. S. Stasinevich and G. A. Egorenko, *Russ. J. Inorg. Chem.*, 1968, **13**, 341–343.
12 P. Martelli, R. Caputo, A. Remhof, P. Mauron, A. Borgschulte and A. Züttel, *J. Phys. Chem. C*, 2010, **114**, 7173–7177.
13 J. Urgnani, F. J. Torres, M. Palumbo and M. Baricco, *Int. J. Hydrogen Energy*, 2008, **33**, 3111–3115.
14 W. Grochala and P. P. Edwards, *Chem. Rev.*, 2004, **104**, 1283–1315.
15 *Handbook of Chemistry & Physics*, 2010–2011.
16 R. A. Varin, T. Czujko, C. Chiu, R. Pulz and Z. S. Wronski, *J. Alloys Compd.*, 2009, **483**, 252–255.
17 S. Orimo, Y. Nakamori and A. Züttel, *Mater. Sci. Eng., B*, 2004, **108**, 51–53.
18 M. Aoki, K. Miwa, T. Noritake, G. Kitahara, Y. Nakamori, S. Orimo and S. Towata, *Appl. Phys. A: Mater. Sci. Process.*, 2005, **80**, 1409–1412.
19 M. Au, A. R. Jurgensen, W. A. Spencer, D. L. Anton, F. E. Pinkerton, S. J. Hwang, C. Kim and R. C. Bowman, *J. Phys. Chem. C*, 2008, **112**, 18661–18671.
20 M. Au, W. Spencer, A. Jurgensen and C. Zeigler, *J. Alloys Compd.*, 2008, **462**, 303–309.
21 Z. Z. Fang, X. D. Kang, P. Wang and H. M. Cheng, *J. Phys. Chem. C*, 2008, **112**, 17023–17029.
22 A. F. Gross, J. J. Vajo, S. L. Van Atta and G. L. Olson, *J. Phys. Chem. C*, 2008, **112**, 5651–5657.
23 X. D. Kang, P. Wang, L. P. Ma and H. M. Cheng, *Appl. Phys. A: Mater. Sci. Process.*, 2007, **89**, 963–966.
24 J. J. Vajo and G. L. Olson, *Scr. Mater.*, 2007, **56**, 829–834.
25 J. J. Vajo, S. L. Skeith and F. Mertens, *J. Phys. Chem. B*, 2005, **109**, 3719–3722.
26 G. L. Xia, Y. H. Guo, Z. Wu and X. B. Yu, *J. Alloys Compd.*, 2009, **479**, 545–548.
27 J. Xu, X. B. Yu, Z. Q. Zou, Z. L. Li, Z. Wu, D. L. Akins and H. Yang, *Chem. Commun.*, 2008, 5740–5742.
28 S. Cahen, J. B. Eymery, R. Janot and J. M. Tarascon, *J. Power Sources*, 2009, **189**, 902–908.
29 P. Ngene, P. Adelhelm, A. M. Beale, K. P. de Jong and P. E. de Jongh, *J. Phys. Chem. C*, 2010, **114**, 6163–6168.
30 M. S. Wellons, P. A. Berseth and R. Zidan, *Nanotechnology*, 2009, **20**, 204022.
31 G. Barkhordarian, T. Klassen, M. Dornheim and R. Bormann, *J. Alloys Compd.*, 2007, **440**, L18–L21.
32 J. F. Mao, X. B. Yu, Z. P. Guo, H. K. Liu, Z. Wu and J. Ni, *J. Alloys Compd.*, 2009, **479**, 619–623.
33 S. Garroni, C. Milanese, A. Girella, A. Marini, G. Mulas, E. Menendez, C. Pistidda, M. Dornheim, S. Surinach and M. D. Baro, *Int. J. Hydrogen Energy*, 2010, **35**, 5434–5441.
34 S. Garroni, C. Pistidda, M. Brunelli, G. B. M. Vaughan, S. Surinach and M. D. Baro, *Scr. Mater.*, 2009, **60**, 1129–1132.
35 T. Czujko, R. A. Varin, Z. Wronski, Z. Zaranski and T. Durejko, *J. Alloys Compd.*, 2007, **427**, 291–299.
36 P. E. de Jongh and P. Adelhelm, *ChemSusChem*, 2010, **3**, 1332–1348.
37 A. Zaluska, L. Zaluski and J. O. Ström-Olsen, *Appl. Phys. A: Mater. Sci. Process.*, 2001, **72**, 157–165.
38 R. A. Varin and C. Chiu, *J. Alloys Compd.*, 2005, **397**, 276–281.
39 Z. Z. Fang, P. Wang, T. E. Rufford, X. D. Kang, G. Q. Lu and H. M. Cheng, *Acta Mater.*, 2008, **56**, 6257–6263.
40 J. Gao, P. Adelhelm, M. H. W. Verkuijlen, C. Rongeat, M. Herrich, P. J. M. Van Bentum, O. Gutfleisch, A. P. M. Kentgens, K. P. De Jong and P. E. De Jongh, *J. Phys. Chem. C*, 2010, **114**, 4675–4682.
41 R. D. Stephens, A. F. Gross, S. L. Van Atta, J. J. Vajo and F. E. Pinkerton, *Nanotechnology*, 2009, **20**, 204018.
42 W. Lohstroh, A. Roth, H. Hahn and M. Fichtner, *ChemPhysChem*, 2010, **11**, 789–792.
43 C. P. Baldé, B. P. C. Hereijgers, J. H. Bitter and K. P. de Jong, *Angew. Chem., Int. Ed.*, 2006, **45**, 3501–3503.
44 R. W. P. Wagemans, J. H. Van Lenthe, P. E. De Jongh, A. J. Van Dillen and K. P. De Jong, *J. Am. Chem. Soc.*, 2005, **127**, 16675–16680.
45 A. Ampoumogli, T. Steriotis, P. Trikalitis, D. Giasafaki, E. G. Bardaji, M. Fichtner and G. Charalambopoulou, *J. Alloys Compd.*, DOI: 10.1016/j.jallcom.2010.10.09.
46 M. Felderhoff, C. Weidenthaler, R. von Helmolt and U. Eberle, *Phys. Chem. Chem. Phys.*, 2007, **9**, 2643–2653.
47 P. Adelhelm, J. B. Gao, M. H. W. Verkuijlen, C. Rongeat, M. Herrich, P. J. M. van Bentum, O. Gutfleisch, A. P. M. Kentgens, K. P. de Jong and P. E. de Jongh, *Chem. Mater.*, 2010, **22**, 2233–2238.
48 M. H. W. Verkuijlen, J. B. Gao, P. Adelhelm, P. J. N. van Bentum, P. E. de Jongh and A. P. M. Kentgens, *J. Phys. Chem. C*, 2010, **114**, 4683–4692.
49 K. J. D. Mackenzie and M. E. Smith, *Multinuclear Solid-State NMR of Inorganic Materials*. Pergamon, 2002.
50 A. D. Irwin, J. S. Holmgren and J. Jonas, *J. Non-Cryst. Solids*, 1988, **101**, 249–254.
51 G. D. Soraru, N. Dallabona, C. Gervais and F. Babonneau, *Chem. Mater.*, 1999, **11**, 910–919.
52 S. J. Hwang, R. C. Bowman, J. W. Reiter, J. Rijssenbeek, G. L. Soloveichik, J. C. Zhao, H. Kabbour and C. C. Ahn, *J. Phys. Chem. C*, 2008, **112**, 3164–3169.
53 V. Stavila, J. H. Her, W. Zhou, S. J. Hwang, C. Kim, L. A. M. Ottley and T. J. Udovic, *J. Solid State Chem.*, 2010, **183**, 1133–1140.
54 R. Caputo, S. Garroni, D. Olid, F. Teixidor, S. Surinach and M. D. Baro, *Phys. Chem. Chem. Phys.*, 2010, **12**, 15093–15100.
55 N. Brun, R. Janot, C. Sanchez, H. Deleuze, C. Gervais, M. Morcrette and R. Backov, *Energy Environ. Sci.*, 2010, **3**, 824–830.
56 P. Ngene, M. van Zwienen and P. E. de Jongh, *Chem. Commun.*, 2010, **46**, 8201–8203.
57 P. Adelhelm, K. P. De Jong and P. E. De Jongh, *Chem. Commun.*, 2009, 6261–6263.
58 X. Ke and I. Tanaka, *Phys. Rev. B: Condens. Matter Mater. Phys.*, 2005, **71**, 024117.
59 J. Šubrt and K. Tobola, *J. Therm. Anal.*, 1976, **10**, 5–12.